IEEE 1989
ULTRASONICS SYMPOSIUM
MONTREAL
OCTOBER 3-6, 1989

ACOUSTIC MICROSCOPY OF CLADDED OPTICAL FIBERS

C.K. Jen, C. Neron, J.F. Bussiere, K. Abe[a], L. Li[b], R. Lowe[c] and J. Kushibiki[d]

IMRI, National Research Council of Canada, Boucherville, Quebec, Canada J4B 6Y4
a) National Optics Institute., Sainte-Foy, Quebec, Canada G1V 4C5
b) Dept. of Elect. and Computer Science, The University, Southampton, U.K. SO9 5NH
c) Optical Cable Div., Northern Telecom Ltd., Saskatoon, Saskachewan, Canada S7K 3L7
d) Department of Electrical Eng., Tohoku University, Sendai, Japan 980

ABSTRACT

Leaky surface acoustic wave velocity (v_{LSAW}) and attenuation (α_{LSAW}) profiles across the diameters of cladded glass fibers or fiber preforms are presented. Optical fibers with different dopants such as GeO_2, F , B_2O_3, etc., and dopant concentrations have been investigated. The role of acoustic profiles across the core and cladding regions in the design of optical fibers for several device applications is outlined. By comparing v_{LSAW} profiles with the corresponding optical refractive index profile, n, the relation between $\Delta v_{LSAW}/v_{LSAW}$ and $\Delta n/n$ is obtained for several dopants. Potential applications of cylindrical glass rods with graded acoustic velocity profiles are also discussed.

I. INTRODUCTION

Coherent optical fiber transmission systems are attractive for realizing long repeater spacing and large transmission capacity. It is important for such systems that the optical spectrum and the intensity of the propagating wave in an optical fiber be narrow and large respectively. In a single mode optical fiber (SMOF), however, stimulated Backward Brillouin scattering (SBBS) can exist with an input power as low as a few milliwatts, and over 60% of the input power goes back to the input end of the fiber owing to SBBS [1]. SBBS may be a serious limitation of input power launching into the fiber [2]; it is then necessary either to operate at power levels below the threshold for SBBS or to reduce the gain of SBBS. SBBS also plays an important role in many optical fiber devices such as fiber ring resonators [3] and narrowband tunable optical filters for channel selection in densely packed wavelength division multiplex optical fiber systems [4].

Pure and doped fused silica glasses are widely used as core and cladding materials for cladded optical fibers. Their acoustic properties are of great importance [5] because: (i) depending on the acoustic velocity profile between the core and the cladding, the threshold of SBBS [1,2] may differ by a factor of fifteen [6] and (ii) acoustically induced phase modulation in single mode optical fibers has been of interest for sensor and telecommunication applications [7,8]. Cladded acoustic fibers [9,10] can also be made of these glasses and the acoustic guidance of the propagating acoustic waves intimately depends on the acoustic profile across the fiber diameter.

Acoustic properties of cladded glass fibers have been studied previously by Brillouin scattering [7,11] and acoustic standing wave resonance methods [8], but only averaged bulk acoustic wave (BAW) velocities could be obtained. Although scanning acoustic microscope images (amplitude) of different types of fibers have been reported [12] which show qualitatively the presence of gradients in acoustic properties, quantitative results were limited by phase reversal phenomena of SAM images [12,13] and by the potentially large error in the determination of acoustic impedance using reflection coefficients (amplitude) at the liquid-solid interface with a highly focussed acoustic beam [14]. In addition, qualitative elastic constants of several different glasses in bulk form have been studied by V(z) curves of a line-focus SAM [15]. In this paper, a V(x,z) analysis using a reflection acoustic microscope operated at 775 MHz is employed to obtain the leaky surface acoustic wave (LSAW) velocity and attenuation profiles across diameters of fibers or fiber preforms. These acoustic profiles are then compared with optical refractive index profiles of cladded fibers.

II. V(x,z) ANALYSIS

Since it is very difficult to obtain the radial distribution of bulk longitudinal, v_L, or shear wave velocity, v_S, for generally small diameter cladded glass fibers, an alternative which uses the reflection scanning acoustic microscopy (SAM) and V(z) technique to obtain v_{LSAW} profile is studied here. The principles of reflection SAM and V(z) curve measurements (where V(z) is the voltage response of the piezoelectric transducer of the SAM lens while the lens is moving toward the sample or vice versa along the lens axis direction, z,) are well documented [16,17]. Our technique records V(z) curves while scanning an arbitrary x-axis along the surface of the sample. A V(x,z) plane is then obtained. Figure 1(a) shows a transmission optical image of a cladded glass fiber consisting of two doped core regions. The optical refractive index profile of this fiber, measured in preform stage (i.e. before fiber drawing) is illustrated in Fig.1(b) for comparison purpose. Figure 2 is the V(x,z) curve measured along a horizontal line across the middle of Fig.1(a). In Fig.2 the horizontal and the vertical axes correspond to x and -z respectively, and the brightness is proportional to V. At each x value one V(z) curve can be displayed along the vertical, -z, axis direction. Figure 3 shows three V(z) curves at three different x positions indicated in Fig.2. The V(z) curve at each x position is processed by a Fourier analysis technique including a Fast Fourier Transform (FFT) [17].

The beat (oscillatory) pattern in Fig.3 gives rise to the bright and dark regions in Fig.2. The distance between the periodic dips is known as Δz. The relation between the velocity, v_{LSAW}, of the leaky surface acoustic wave (LSAW) and Δz is given as [17]

$$v_{LSAW} = v_w/[1 - (1 - v_w/2f\Delta z)^2]^{1/2} \qquad (1)$$

where v_w is the velocity of the water couplant and f is the ultrasonic frequency (775 MHz). For our samples larger Δz

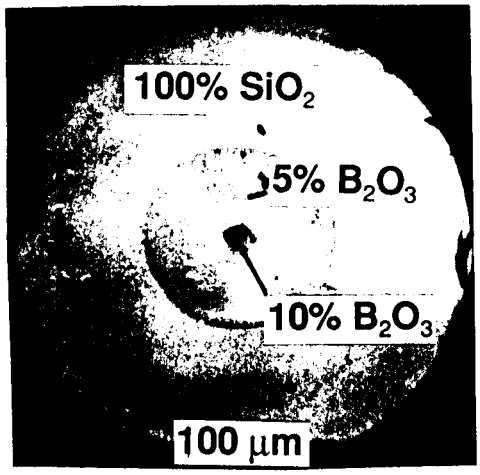

(a)

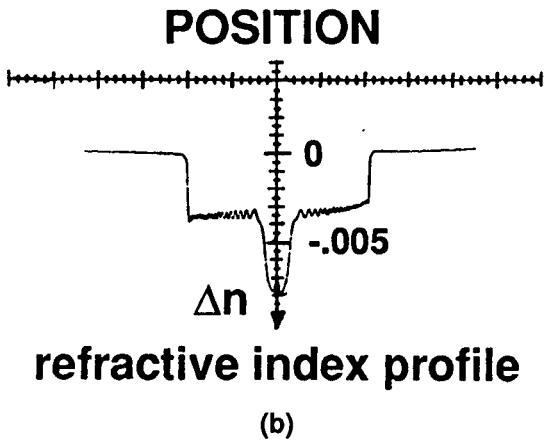

(b)

Fig.1 (a) Transmission optical micrograph of a cladded fiber,(b) optical refractive index profile.

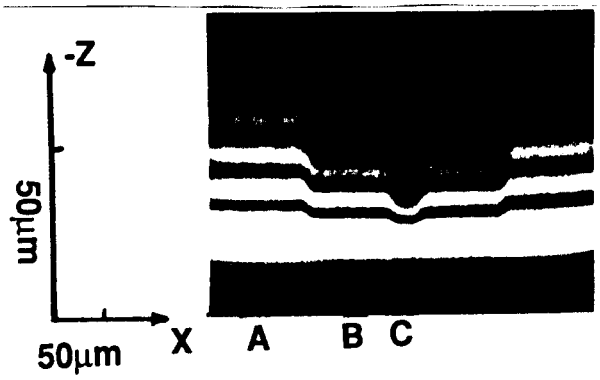

Fig.2 V(x.z) plane across the center of fiber in Fig.1(a).

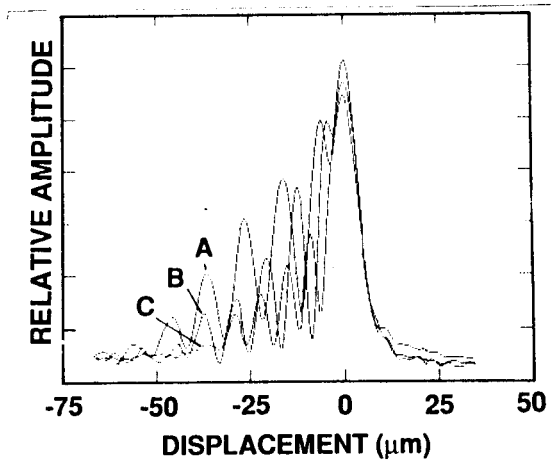

Fig.3 V(z) curves obtained at three different x positions shown in Fig.2. on : A: 100% SiO_2, B: 5% B_2O_3 and C: 10% B_2O_3.

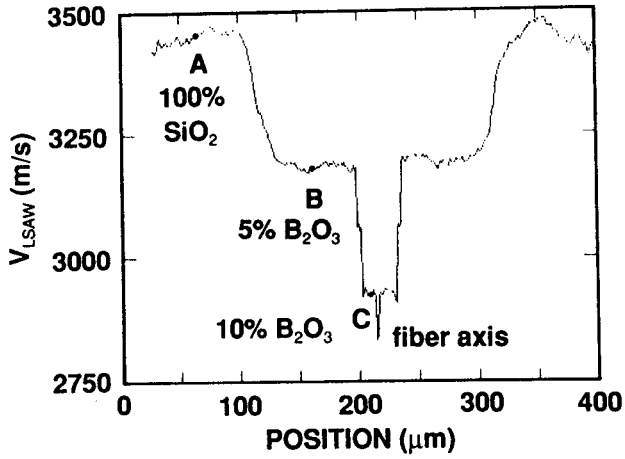

(a)

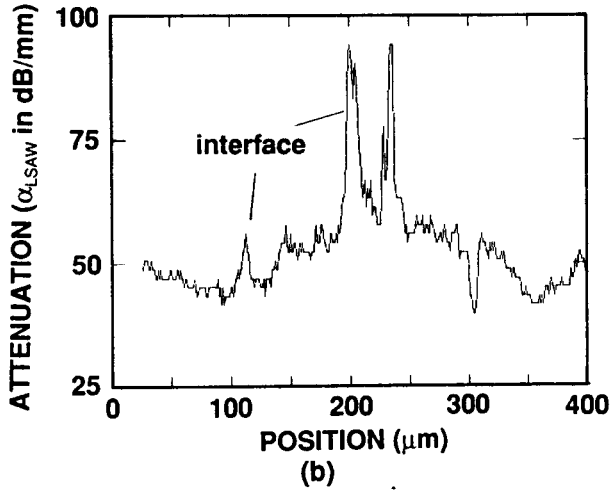

(b)

Fig.4 (a) v_{LSAW} and (b) α_{LSAW} profiles.

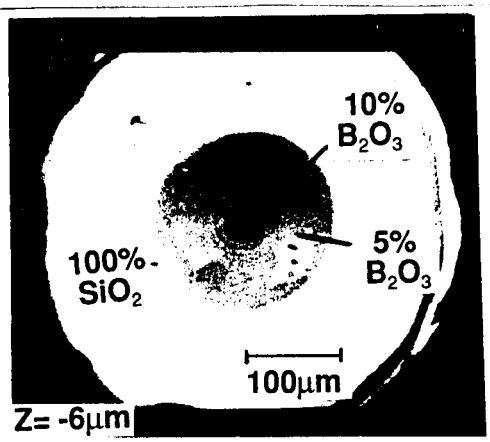

Fig.5 Acoustic micrograph at z = -6μm.

refers to higher v_{LSAW}.

Before the FFT processing, the low frequency background of the V(z) curve (arising from the SAM lens response) must be removed. Usually, this is performed using a calibration procedure of the lens with the help of a material such as lead or teflon which supports no leaky surface wave [17]. In our experiments, we used a different approach, where the low frequency backgound was removed with a high pass numerical filter, consisting of a first order differentiation of the V(z) curves [18]. After the FFT processing of this trace the spatial frequency spectrum versus the wavenumber k (rad/μm) is obtained. The v_{LSAW} can be then deduced from the wavenumber at the peak of this spectrum, and the attenuation α_{LSAW} of the LSAW from the width of this spectrum [17]. The v_{LSAW} and α_{LSAW} profiles deduced from the V(x,z) curves shown in Fig.2 are given in Figs.4(a) and 4(b) respectively. The relative accuracy of v_{LSAW} and α_{LSAW} measurements is limited to approximately 1% and 10 dB/mm respectively, due to the imperfect fiber polishing. At boundaries between two regions of different elastic properties, a reduced measurement accurary was observed. Since the contrast of acoustic images among regions of different elastic properties changes with -z position (phase reversal phenomena [12,13]), only one image obtained, at z = -6 μm, is given in Fig.5 as a reference. From Fig.2 this phenomenon can be verified. For instance, at each different -z, the image constrast along the scanned x-line corresponds to the contrast of V(x,z).

III. ACOUSTIC PROPERTIES OF SEVERAL MULTILAYERED GLASS FIBERS

Fiber A shown in Fig.1(a) was used as a demonstration for the V(x,z) analysis in the previous section. Before the SAM studies, all fiber end surfaces were polished. The resolution of the 775 MHz SAM at its focus is 2 μm, but due to the defocussing mechanism during V(z) measurements, v_{LSAW} and attenuation profiles, shown in Figs.4(a) and 4(b) respectively, at a particular x_0 position are averaged values around x_0, which extend over a region of ~ 10 μm diameter. Therefore at the boundary between different dopant concentrations the variation of v_{LSAW} profiles is not as sharp as observed for the optical refractive index distribution.

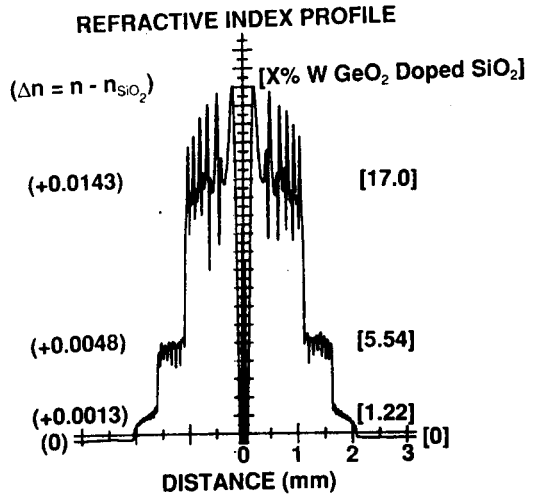

Fig.6 Refractive index profiles of fiber preforms with dopants GeO_2.

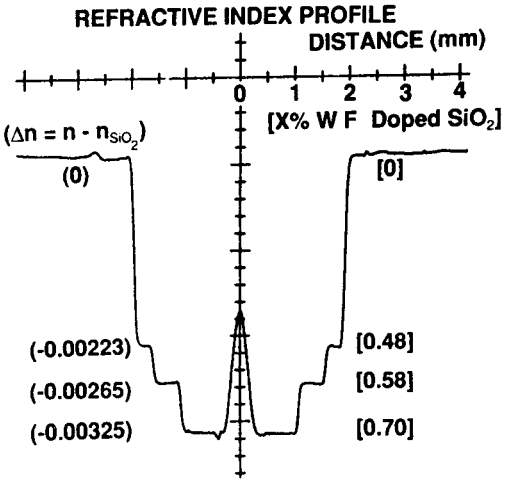

Fig.7 Refractive index profiles of fiber preforms with dopants F .

In addition to Fiber A, fiber preforms B and C shown in Figures 6 and 7 were made in order to obtain some quantitative relation given in Table I betweem the dopant concentration and the variation of n (Δn) and v_{LSAW} (Δv_{LSAW}). Dopants B_2O_3, GeO_2 and F were chosen because they are commonly used as cladding and core materials respectively. They were also used in the SBBS measurement in Refs.[6,19]. For GeO_2, because it is very difficult to produce a smooth profile, only the averaged value in the middle at each "step" indicated by the dopant concentration in the refractive index profile shown in Fig.6 are used. The averaging method for V(x,z) curves was explained in Ref.[18].

As Indicated in Table I the effect of the various dopants studied is to cause a decrease of v_{LSAW} with respect to pure fused silica. The above observations on the tendency of the variation of v_{LSAW} is consistent with reported bulk longitudinal, v_L, and shear wave velocity ,v_S, data collected in Ref.[20]. For instance, B_2O_3 dopant reduces v_L and v_S, and also v_{LSAW}. It is believed that v_L and v_S profiles could be used as acoustic design

Table I Variation of v_{LSAW} and n for Different Dopants and Dopant Concentrations

DOPANTS	AMOUNT (%)	Δn (%)	Δv_{LSAW} (m/s) (%)
SiO_2	100	0 (0)	0 (0)
B_2O_3	5	-0.0035 (-0.24)	-270 (-7.8)
B_2O_3	10	-0.0075 (-0.51)	-525 (15.2)
GeO_2	1.22	+0.0013 (+0.09)	-80 (2.3)
GeO_2	5.54	+0.0048 (+0.33)	-155 (-4.5)
GeO_2	17.0	+0.0143 (+0.97)	-330 (-9.6)
F	0.48	-0.00223 (-0.15)	-47 (-1.36)
F	0.58	-0.00265 (-0.18)	-63 (-1.83)
F	0.70	-0.00325 (-0.22)	-76 (-2.2)

criteria for optical and acoustic fibers [5], and it is expected that the v_{LSAW} profile may be used as a practical alternative. In Table I it is also noted that the rate of change in Δv_{LSAW} is different than that of Δn.

It is very interesting to note that a sharp dip in the measured v_{LSAW} shown in Fig.4(a) is observed at the fiber axis. A similar abrupt variation also appears in the refractive index profile shown in Fig.1(b). This dip region is commonly produced during the collapsing process of fiber preform fabrication involving modified chemical vapor deposition [21]. Figure 4(b) indicates that the α_{LSAW} is higher at the interface between two regions of different dopant concentrations. The main reason is that the acoustic scattering occurs at this interface because of the elastic discontinuity. As expected α_{LSAW} of pure fused silica regions is less than that of regions having dopants. Further studies on the effects of α_{LSAW} on the performance of optical and acoustic fibers will be performed.

IV. GRADED INDEX GLASS RODS

Graded refractive index distributions are commonly adopted in multimode optical fiber designs for the purpose of dispersion reduction [22]. We used graded index glass rods as samples for the SAM study. In fact, glass optical rods with a parabolic profile are generally named GRIN lens and widely used. GRIN lenses may be produced with a graded index of refraction along the radial or axial direction. Only the former type is demonstrated here. The parameters that define the index distribution provide valuable new degrees of freedom for designers of optical imaging systems. They can be expressed as

$$n(r) = n_0 [1 - (A/2)r^2] \qquad (2)$$

where n_0 is the refractive index at the rod axis, A is a positive constant and r is the radial distance from the axis.

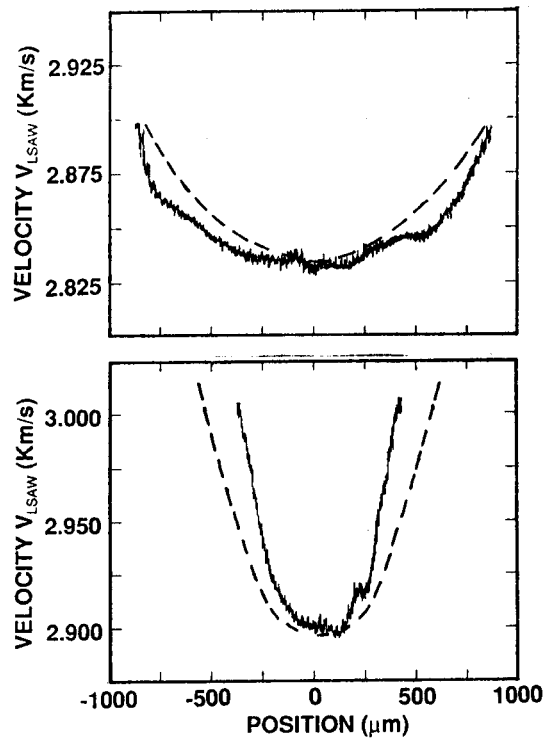

Fig.8 v_{LSAW} profile (solid lines) of GRIN rods with $\sqrt{A}$ equal to 0.247 (upper curve) and 0.499 (lower curve). The refractive index variation is given in dashed lines.

Figures 8 shows v_{LSAW} distributions across the diameters of two GRIN lenses (from Melles Griot) with $\sqrt{A}$ equal to 0.247 (upper solid curve) and 0.499 (lower solid curve). It clearly demonstrates that these two GRIN rods also provide graded v_{LSAW} profiles. It is noted that these two lenses have different n_o's. The variation of v_{LSAW} appears sharper in the GRIN rod with a larger A. Because GRIN rods are commonly made of multidopants [23] and the refractive index contribution of each dopant is not the same as v_{LSAW}, the v_{LSAW} profile does not follow the same parabolic form of optical refractive index distribution as shown in the dashed lines in Fig.8. For the the lens with $\sqrt{A} = 0.247$ the rate of change in v_{LSAW} is slower than that of n, but it is reverse for the lens with $\sqrt{A} = 0.499$. The non smoothness of the v_{LSAW} profile is mainly due to our measurement accuracy. However the graded acoustic velocity profile can provide a mechanism for acoustic focussing in GRIN rods. Novel acoustic lenses may thus be constructed because of the freedom in introducing the desired profile. In nondestructive evaluation of materials long buffer rods are sometimes required. The undesired beam spreading may be minimized in a long rod with a proper graded acoustic velocity profile. A detailed discussion on acoustic properties of GRIN lenses will be reported elsewhere [24]. It is important to note that the measured v_{LSAW} at a particular radial position of GRIN lenses is an average value over the diameter of the focused acoustic beam (10 μm in our case). For more precise measurements of v_{LSAW} profiles especially at regions of sharp variation, a higher frequency of operation is necessary.

V. DISCUSSION AND CONCLUSION

A V(x,z) analysis with a reflection scanning acoustic microscope operated at 775 MHz has been used to obtain the leaky surface acoustic wave velocity v_{LSAW} and attenuation profiles of cladded glass fibers of different dopant and dopant concentrations. It has been shown that for all the samples studied the effect of added dopants on the variation of bulk acoustic wave properties of pure fused silica has the same tendency as that on v_{LSAW}. Therefore v_{LSAW} profiles could be used as an alternative acoustic design criterion for optical and acoustic fibers. We have also demonstrated that glass rods with graded refractive index distributions may also have graded acoustic velocity profiles. These rods may be used as acoustic lenses having the advantage of a flat end surface [24].

In addition to all optical guidance requirements, in order to transmit more optical power in the fiber core, the acoustic properties of the core and cladding of SMOF should be chosen in such a way that the acoustic guidance in the fiber core is minimized; thus less SBBS will take place. Making v_s and v_L of the core higher than those of the cladding is one approach. As the velocity difference increases, the threshold of SBBS increases and the SBBS gain decreases. This approach can be verified by the experimentally observed high threshold of SBBS in a fiber with pure fused silica as core and B_2O_3 doped fused silica as cladding [6]. This fiber does not guide acoustic waves well. It is also noted in Ref.[3] that the SBBS threshold of a SMOF can be as low as 65 μWatt optical power in the fiber core. However, in certain applications where an optical fiber having high SBBS may be desirable [4], then good acoustic wave guidance is necessary.

REFERENCES

[1] D. Cotter, "Stimulated Brillouin scattering in monomode optical fibers", J. Opt. Comm., Vol.1, pp.10-19, 1980.

[2] R.G. Smith, "Optical power handling capacity of low loss optical fibers as determined by stimulated Raman and Brillouin scattering", Appl. Opt. Vol.11, pp.2489-2494, 1972.

[3] R. Kadiwar and I.P. Giles, "Effects of stimulated Brillouin scattering on the performance of polarization maintaining all-fiber ring resonators", Optics Lett., Vol.14, pp.332-334, 1989.

[4] A.R. Chraplyvy and R.W. Tkach, "Narrowband tunable optical filter for channel selectrion in densely packed WDM systems", Electron. Lett., Vol.22, pp.1084-1085, 1086.

[5] C.K. Jen, J.E.B. Oliveira, N. Goto and K. Abe, "Role of guided acoustic wave properties in single-mode optical fiber design", Elect. Lett., Vol.23, pp.1419-1420, 1988.

[6] R.H. Stolen, "Polarization effects in fiber Raman and Brillouin lasers", IEEE J. Quantum Electron., Vol.QE-15, pp.1157-1160, 1979.

[7] N. Lagakos, J.A. Bucaro and R. Hughes, "Acoustic sensitivity predictions of single mode optical fibers using Brillouin scattering", Appl. Opt., Vol.19, pp.3668-3670, 1980.

[8] F.S. Hickernell, "The characteristics of coaxial ZnO thin-film BAW transducers on optical fibers", Proc. IEEE Ultrasonics Symp., pp.417-420, 1988.

[9] A. Safaai-Jazi, C.K. Jen and G.W. Farnell, "Analysis of weakly guiding fiber acoustic waveguides", IEEE Trans. Vol.UFFC-32, pp.59-68, 1986.

[10] C.K. Jen, A. Safaai-Jazi and G.W. Farnell, "Leaky modes in weakly guiding fiber acoustic waveguides", IEEE Trans. Vol.UFFC-32, pp.634-643, 1986.

[11] N. Shibata, R.G. Waarts and B.-P. Braun, "Brillouin gain spectra for single mode fibers having pure silica, GeO_2 doped, P_2O_5 doped cores", Opt. Lett, Vol.12, pp.269-271, 1987.

[12] C.K. Jen, G.W. Farnell, R.D. Kinsella and J.F. Bussiere, "Elastic profile measurement of optical fibers via reflection acoustic microscopy", Elect. Lett., Vol.19, pp.922-924, 1983.

[13] R.D. Weglein, "A model for predicting acoustic material signatures", Appl. Phys. Lett., Vol.34, pp.179-181, 1979.

[14] K.K. Liang, "Accuracy of acoustic impedance determination using a focusing beam", Proc. IEEE Ultrasonics Symp., pp.1141-1146, 1987.

[15] J. Kushibiki, T. Ueda and N. Chubachi, "Determination of elastic constants by LFB acoustic microscope", Proc. IEEE Ultrasonics Symp., pp.817-821, 1989.

[16] A. Atalar, "An angular spectrum approach to contrast in reflection acoustic microscopy", J. Appl. Phys., pp.5130-5139, 1978.

[17] J. Kushibiki and N. Chubachi, "Material characterization by line focus beam acoustic microscope", IEEE Trans. Sonics and Ultrason., Vol.SU-32, pp.189-212, 1985.

[18] J.Y. Duquesne, K. Yamanaka, C. Neron, C.K. Jen, L. Piche and G. Lessard, "Study of spherulites in a semi-crystalline polymer using acoustic microscopy", to appear in Proc. of Materials Res. Soc. Conf. Symp.U: Nondestructive Characterization of Materials, Boston, Nov. 1988.

[19] N. Shibata, K. Okamoto and Y. Azuma, "Longitudinal acoustic modes and Brillouin gain spectra for GeO_2 doped core single mode fibers", J. Opt. Soc. Am. B, Vol.6, pp.1167-1174, 1989.

[20] C.K. Jen, "Similarity and differences between fiber acoustics and fiber optics", Proc. IEEE Ultrasonics Symp., pp.1128-1133, 1985.

[21] W.G. French, R.E. Jaeger, J.B. Macchesney, S.R. Nagel, K. Nassau and A.D. Pearson, "Fiber preform preparation", in "Optical Fiber Telecommunications", S.E. Miller and A.G. Chynoweth eds, Academic Press, N.Y., pp.233-261, 1979.

[22] T. Uchida, M. Furukawa, I. Kitano, K. Koizumi and H. Matsumura, "Optical Characteristics of a light-focusing fiber guide and its application", IEEE J. Quantum. Elect., Vol.QE-6, pp.606-612, 1970.

[23] Marchand, E.W.: 'Gradient Index Optics', Academic Press, New York, 1978.

[24] C.K. Jen, A. Safaai-Jazi, C. Neron and J.C.H. Yu, to be published.